Accepted Manuscript

Effect of semi-solid forging on microstructure and mechanical properties of in-situ cast Al-Cu-TiB_2 composites

James Mathew, Animesh Mandal, S. Deepak Kumar, S. Bajpai, M. Chakraborty, G.D. West, Prakash Srirangam

PII: S0925-8388(17)31313-0

DOI: 10.1016/j.jallcom.2017.04.113

Reference: JALCOM 41517

To appear in: *Journal of Alloys and Compounds*

Received Date: 17 January 2017

Revised Date: 28 March 2017

Accepted Date: 12 April 2017

Please cite this article as: J. Mathew, A. Mandal, S.D. Kumar, S. Bajpai, M. Chakraborty, G.D. West, P. Srirangam, Effect of semi-solid forging on microstructure and mechanical properties of in-situ cast Al-Cu-TiB_2 composites, *Journal of Alloys and Compounds* (2017), doi: 10.1016/j.jallcom.2017.04.113.

Effect of semi-solid forging on microstructure and mechanical properties of in-situ cast Al-Cu-TiB_2 composites

James Mathew[1], Animesh Mandal[2], S. Deepak Kumar[3], S. Bajpai[4], M. Chakraborty[5], G.D. West[1], Prakash Srirangam[1*]

[1] Warwick Manufacturing Group, University of Warwick, Coventry, CV4 7AL, UK

[2] School of Minerals, Metallurgical and Materials Engineering, Indian Institute of Technology, Bhubaneswar, India

[3]School of Mechanical Sciences, Indian Institute of Technology, Bhubaneswar, India

[4]Advanced Materials Technology Department, CSIR-Institute of Minerals and Materials Technology, Bhubaneswar, India

[5]ADAMAS University, Barasat, Kolkata, West Bengal, India

* Corresponding author: p.srirangam@warwick.ac.uk (P. Srirangam)

Key words:
Al-Cu alloys, metal matrix composite, semi-solid forging, TiB_2 particles, EBSD, nano-indentation, Dynamic recrystallization

Abstract:

The present work deals with the effect of semisolid processing on microstructure and mechanical properties of Al-4.5 % Cu – 5% TiB_2 in-situ cast composites. The composite was prepared by flux assisted synthesis in which TiB_2 particles were formed in-situ through an exothermic reaction between K_2TiF_6 and KBF_4 halide salts. Al-4.5wt% Cu alloy and Al-4.5% Cu-5 % TiB_2 composite samples were forged in semisolid state with 0.3 volume fraction of liquid. Semisolid forging was carried out for two forge reductions (30% and 50% forge reductions). Microstructure studies show that the semi-solid forging results in uniform distribution of TiB_2 particles and Al_2Cu particles in the composite. Further, TiB_2 particles play a dual role as grain refiners as well as reinforcements of composites. EBSD and nano indentation studies shows that semisolid forging results in dynamic recrystallization of grains in the composite with significant grain refinement which leads to a marked increase in hardness and elastic modulus of the alloy as well as the composite.

1. Introduction

The demand for lightweight and low cost dispersion strengthened components is increasing in automotive and aerospace applications to improve the fuel efficiency and to reduce greenhouse gas emissions [1][2]. An important challenge in manufacturing of light weight and high strength aluminium parts is to produce near net shape components of complex geometry with desired properties meeting the requirements of automotive applications [1]. As a result, there is a considerable interest in aluminium based metal matrix composites (MMCs) due to their high specific strength and stiffness [3]. In-situ metal matrix composites in which reinforcement is generated within the alloy offers an advantage of clean interface with minimal interfacial reaction between reinforcement and matrix [4][5]. Amongst many types of reinforcements used [3, 6-13], TiB_2 reinforcement in aluminium alloys using salt based in-situ methods offers great advantages such as minimal reactivity[7], clean interface[14], sound thermal conductivity [15] and high elastic modulus and hardness [16]. TiB_2 particles acts as a heterogeneous nucleating site for α-Al [11] controlling the grain size, thereby improves the mechanical properties of the Al matrix. During solidification this sub- micron sized TiB_2 particles are pushed to the grain boundaries resulting in the formation of clusters [17]. Unfortunately, the clustered second phase particles cannot control the grain size [17]. These clusters could be fragmented and the particle distribution could be improved by secondary processes such as extrusion, rolling and semisolid rolling or forging [16, 18-21]. The semi-solid forming results in a non-dendritic microstructure due to forming at a temperature between solidus and liquidus temperature [22]. In semisolid state, the enclosed liquid component allows the slip and rotations of solid grains thereby improving the formability of metals [23]. In addition to this, semisolid temperature has a critical role on the final microstructure such as grain orientation, grain morphology and distribution of reinforcement particles during solidification of alloys [24]. Liu et al. [25] reported that the semisolid

processing has a significant effect on improvement of mechanical properties of the alloys. The study of semi-solid forging on aluminium alloys has showed a high-temperature dependence on microstructure, especially on precipitation in Al-Cu alloys [26]. Higher amounts of solid fraction are usually preferred as they reduce porosity, promote laminar flow of liquid, and also improve the surface quality of alloys [24]. Previous research studies on semisolid deformation behaviour of metals have shown that a liquid fraction between 10% and 30% is commonly suitable for semi-solid forging [27].

Recent X-ray computed tomography studies on Al-4.5%Cu-5%TiB_2 in-situ composite showed that semisolid forging has resulted in improvement of TiB_2 particle size distribution and reduction of particle clusters [28]. Additionally, Deepak Kumar et al. [29], suggested that semisolid forging of Al-5TiB_2 composites improves mechanical properties of the composite. Aluminium alloys are generally expected to produce new grains during hot deformation by dynamic recrystallization process which can be experimentally studied using [30, 31]. Electron backscattered diffraction (EBSD) mapping of grain boundary misorientation [32]. It was found that only few studies have used EBSD investigation of semisolid processed Al-TiB_2 composites [33] and there is no earlier report on EBSD studies on semisolid forged Al-4.5% Cu - 5% TiB_2 in-situ composites. Since the hardness and Young's modulus behaviour of Al-TiB_2 composites are found to be increased with increased volume fraction of TiB_2 and uniform distribution of TiB_2 particles [34], the semisolid forging would definitely have an influence on the mechanical properties of composites. The effect of semisolid forging on Young's modulus and hardness of Al-TiB_2 composite are important inputs for micro-structure based modelling of the process [35]. Nano indentation studies were rarely carried out on Al-TiB_2 composites to determine Young's modulus and hardness by means of accurately measured load-depth data [36]. In this work, we studied the effect of semi-solid forging on microstructure and mechanical properties of Al-4.5%Cu-5%TiB_2 in-situ composites

thixoforged at 0.3 volume fraction (V_{fl}) of liquid with two forge reductions (30% reduction and 50% reduction).

2. Experimental procedure

2.1 Processing of Al-4.5Cu-5wt%TiB_2 in-situ composite

Al-4.5%Cu-5wt%TiB_2 composite was synthesized by Flux Assisted Synthesis (FAS) technique which consists of addition of halide salts, K_2TiF_6 and KBF_4, to molten Al-4.5Cu alloy at 800 °C and a reaction time of one hour. The schematic of flux assisted synthesis of in-situ Al-Cu-TiB_2 composites is shown in fig 1. The exothermic reaction within the melt results in the formation of titanium-diboride (TiB_2) particles within the matrix. The melt was stirred intermittently every 10 minutes to ensure complete reaction of salts with molten aluminium and homogenous distribution of TiB_2 particles. After completion of reaction, the lighter dross was decanted and the melt was degassed using C_2Cl_6. The composite melt was finally poured into rectangular mild steel mould and machined to dimension of 10 mm x 10 mm x 60 mm prior to forging in semi-solid state. Thixoforging was carried out using 80-ton hydraulic press, at a load of 150 Kg/cm^2 and at a ram speed of 20 mm/sec. As-cast alloy and composite were subjected to forging at 30% and 50% deformation in semi-solid state. As-cast alloy and the composite were forged at 631°C and 632°C respectively corresponding to a liquid fraction of 0.3. The samples were soaked at forging temperature for 10 minutes prior to forging. The K-type thermocouples were used to monitor the temperatures with an accuracy of ± 2 °C.

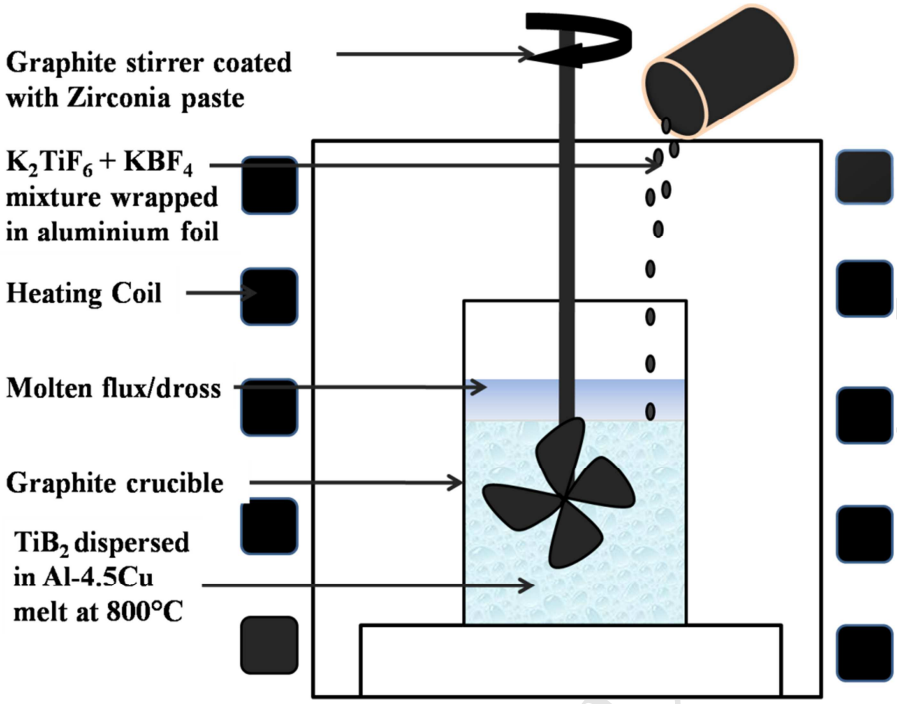

Fig. 1. Schematic of flux assisted synthesis of in-situ Al-Cu-TiB_2 composites

2.2 Microstructural characterization

Microstructure studies of alloy and composite were carried out using optical microscopy and field emission scanning electron microscope (FESEM) after polishing respective samples using standard metallographic procedures. Polished samples were anodised with a Barker's reagent (1.8% HBF_4 in water) applying 23V DC for upto 1 minute. Dark field and bright field micrographs were captured using a NIKON (Model: ECLIPSE LV150N) metallurgical microscope. Grain size analyses was performed as per ASTM E112 standard test method in polarized mode using a LEICA metallurgical microscope (Model: DM 4000M). Samples were deep etched with 20% NaOH solution to study the clustering behaviour of particles at high magnifications using SEM coupled with energy dispersive X-ray spectrometer (Carl Zeiss SMT AG).

2.3 Mechanical property characterization

Nano-indentation tests were performed using a nano-indentation instrument (Fischer-Cripps, Australia) with a standard Berkovich indentor which measures force and displacement as indentation progresses. The Berkovich indenter has a trigonal pyramidal shape with a nominal angle of 65.3°. The samples were ultrafine polished to avoid surface roughness effects on the results of nano indentation studies. For each sample, ten indentations were made using a maximum load of 30 mN with each indentation separated by 20 μm. Details about nano indentation test methodology can be found elsewhere [37]. Fig. 2 shows the typical loading – unloading curves obtained from nano indentation studies [38]. As shown in Fig. 2, P_{max} represents the load at maximum indentation, h_{max} is the indenter displacement at peak load, h_f is the final depth of the contact impression after unloading. The total displacement (h_{max}) is the displacement of the indenter from its initial position at peak load (P_{max}). However, the material elastically recovers its shape partially, when the indenter is unloaded [37-40]. So the total displacement is composed of both elastic and plastic displacements. From this, elastic displacements can be measured to calculate the elastic modulus, E. The hardness, H can be calculated by removing this elastic contribution from the total displacement.

The hardness H can be calculated as;

$$H = \frac{Pmax}{A} \quad (1)$$

Where $P_{max}$is the peak load, A is the projected area of contact between the indenter and sample [38].

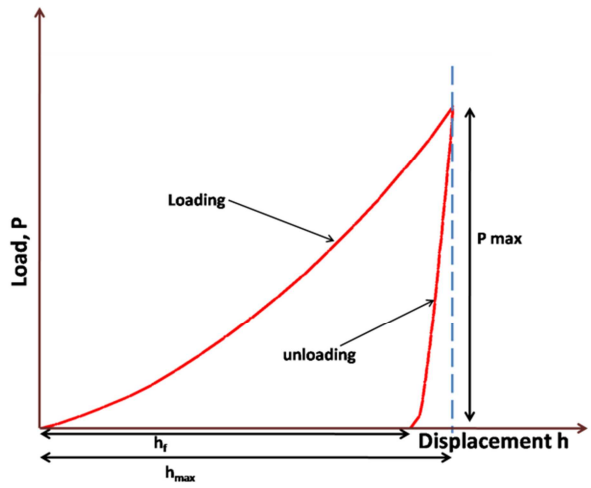

Fig. 2. Schematic representation of a loading-unloading curve

3. Results and discussion

3.1 Microstructure of Al-4.5Cu alloy and Al-4.5Cu-5wt%TiB_2 in-situ composite

Fig. 3 shows the optical microstructure of as cast and semi solid processed Al-4.5Cu alloy and in-situ Al-Cu-TiB_2 composites. As represented in Fig. 3(a), the microstructure of the as cast Al-4.5Cu alloy shows coarse rosette shaped α-Al grains and Al_2Cu dispersed in the alloy. As shown in Fig. 3(b, c), deformation of the alloy in semi-solid state led to a fragmentation and dispersion of Al_2Cu particles (bright phase) . Further, it was observed that higher percentage of deformation (50% reduction) did not lead to enhanced distribution of Al_2Cu particles as shown in Fig 3(c)

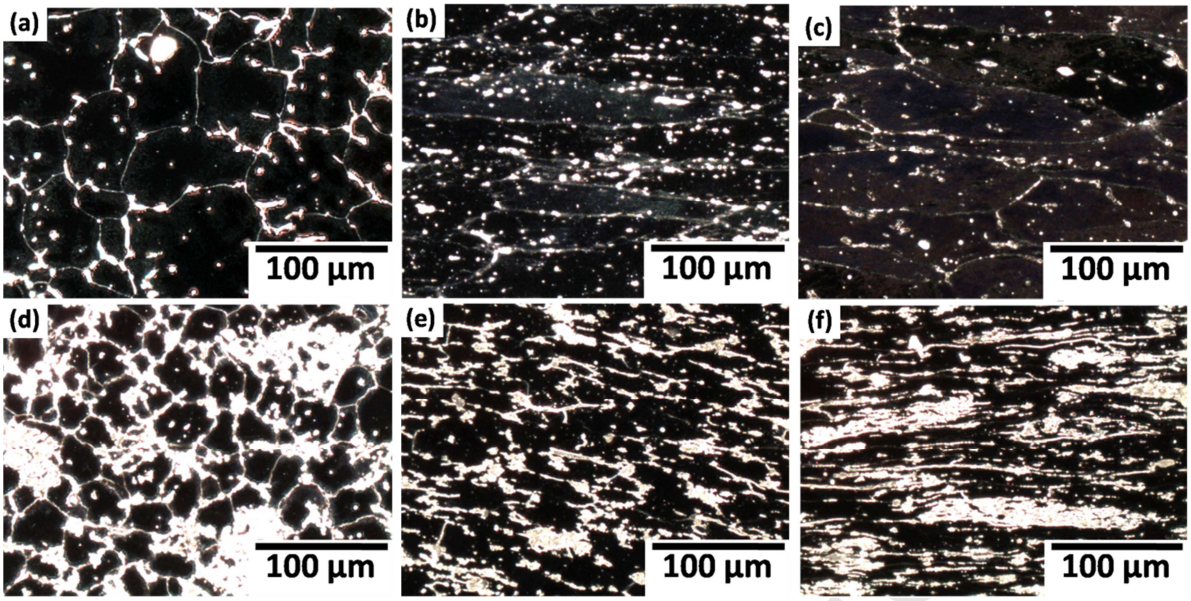

Fig. 3. Dark field optical microstructure of Al-4.5Cu alloy (a) as cast condition (b)$V_{f,\ liquid}$ = 0.3, 30% reduction (c) $V_{f,\ liquid}$ = 0.3, 50% reduction, Al-4.5Cu-5TiB_2 composite (d) as cast condition (e)$V_{f,\ liquid}$ = 0.3, 30% reduction (f) $V_{f,\ liquid}$ = 0.3, 50% reduction

Fig. 3(d) shows the formation of fine α-Al grains in Al-4.5Cu-5TiB_2 composite due to *in-situ* formed TiB_2 particles which act as heterogeneous nucleation sites.TiB_2 is mainly seen in the form of clusters of varying size randomly distributed in the matrix. When samples were subjected to semisolid forging, it is observed that α-Al grains are elongated in the direction normal to forging [Fig. 3(e, f)]. Also, the large agglomerates of TiB_2 particles are fragmented into relatively smaller agglomerates and uniformly distributed in the matrix. The compressive force applied during forging resulted in separation of TiB_2 particle clusters and probably closure of pores in the composite [28]. TiB_2 particles are redistributed by both viscous flow of liquid and fragmentation of unmelted solid grains due to the force applied during semisolid state forging. It was also observed that TiB_2 particles are driven from their original locations at grain boundaries by viscous drag of intergranular liquid when subjected to thixoforging. The composite deformed by 50% [Fig. 3f] shows folds normal to direction of forging.

The α-Al grains in the microstructure of as cast alloy and composites were studied using polarised optical microscopy to understand the effect of semisolid forging on grain refinement Al-4.5 Cu alloy. Fig. 4 shows average grain size of as cast Al-4.5Cu alloy and Al-4.5Cu-5TiB_2 composite. The average grain size of as cast Al-4.5 Cu alloy was found to be 59 µm, while in and as cast Al-4.5Cu-5TiB_2 composite was 24 µm. This shows that fine and uniform grain structure is formed in the composite sample as compared to as-cast alloy due to the presence of TiB_2 particles which acts as grain refiners as well and reinforecement in Al-4.5Cu-5TiB_2 composite.

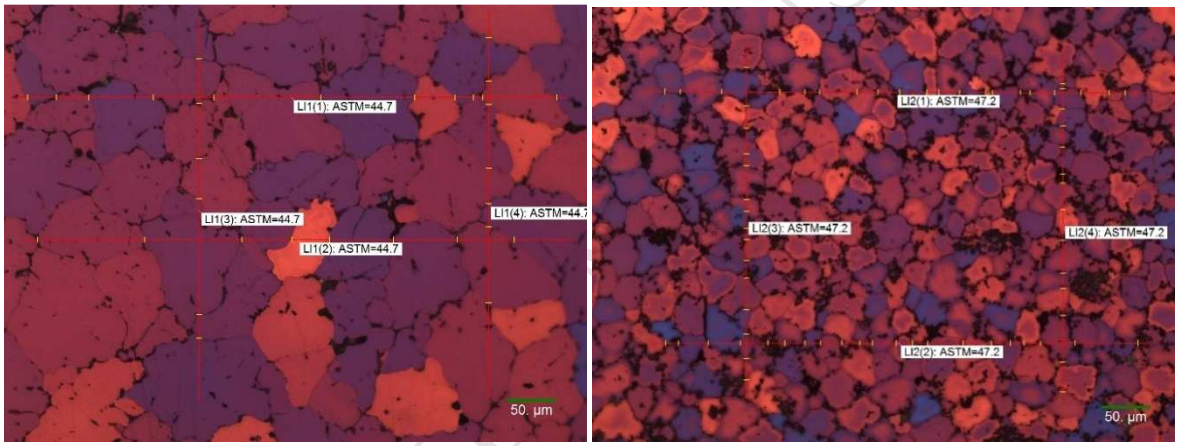

Fig. 4. Polarized optical microstructure of as cast (a) Al-4.5Cu alloy (b) Al-4.5Cu-5TiB_2 composite

In order to understand the effect of semisolid forging on particle clustering and distribution in as cast and semi solid processed in-situ Al-Cu-TiB_2 composites, SEM studies were performed at higher magnifications. Fig. 5 shows SEM images of deep etched as cast and semi solid processed in-situ Al-Cu-TiB_2 composites. As shown in Fig. 5(a), the average size of TiB_2 particle was found to be 1-2 µm in as cast composite. The shape of TiB_2 particles were observed as flakes as well as hexagonal shaped as shown in fig 5(a), which in a close observation seems to have a third dimension. It implies that the particles have a hexagonal

shape in 3 Dimension, but show different face in 2 Dimensional images. Similar observations were made by Sun et al [41] that TiB_2 particles in Al matrix exhibits hexagonal shapes with smooth surfaces. Upon semisolid forging, TiB_2 particles were fragmented and observed to be finer in size as compared to as-cast samples as shown in Fig. 5(b). However, it is to be noted that the TiB_2 particles were embedded in Al_2Cu clusters in the composite as shown in fig 5(b). These clusters were observed to be elongated and distributed in the direction normal to forging along the grain boundaries instead of forming large agglomerates in the matrix.

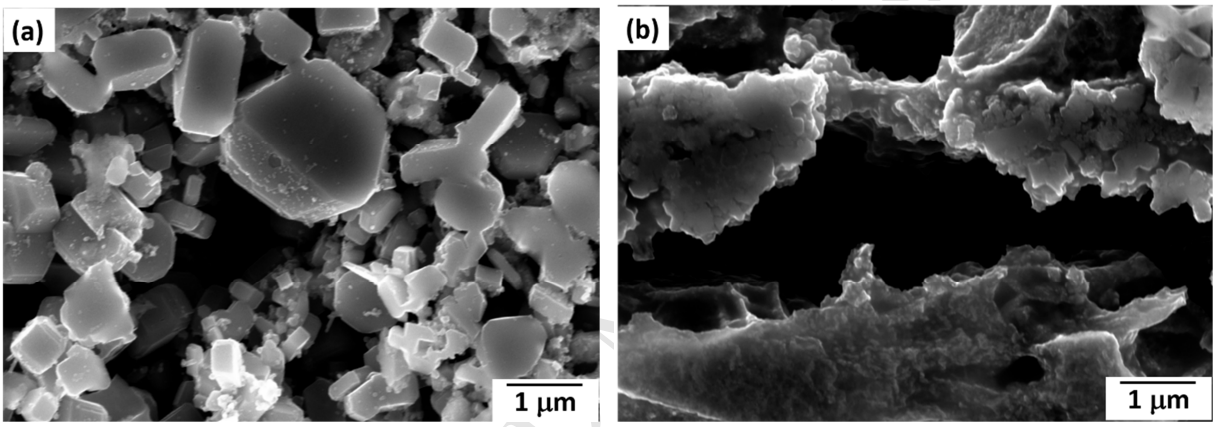

Fig. 5. FESEM Electron backscatter image showing the particle clusters in Al-4.5Cu-5TiB_2 composite (a) as cast condition (b) $V_{f,\ liquid}$ = 0.3, 30% reduction.

3.2 X-Ray Diffraction analysis

Fig. 6 shows the XRD pattern obtained from the Al-4.5Cu-5TiB_2 composite with 0.3 volume fraction of liquid and 30% reduction condition. The intensity peaks corresponding to TiB_2, Al_2Cu and Al represents their presence in the matrix.

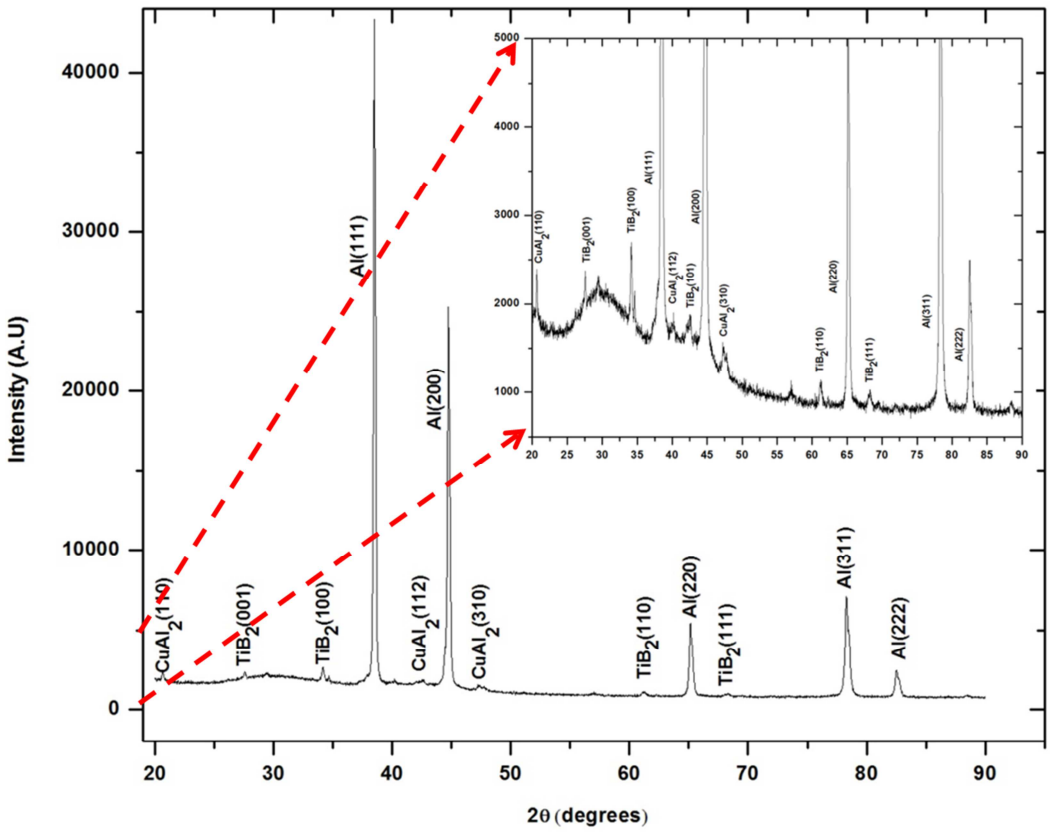

Fig. 6. XRD pattern of Al-4.5Cu-5TiB_2 composite with 0.3 volume fraction of liquid and 30% forge reduction.

3.3 EBSD analysis

Semisolid forging is a material deformation process at semsolid temperature range and is expected to have a dynamic recrystallisation during the process. The α-Al grains in the microstructure of as cast and semi solid processed in-situ Al-Cu-TiB_2 composites were analysed using EBSD to understand the grain orientation, grain boundary characteristics and grain size distribution due to semisolid forging. Fig. 7 shows the grain orientaion in as cast and semi solid processed in-situ Al-Cu-TiB_2 composites. It is to be noted that TiB_2 particles were not able to be identified in EBSD maps due to their extremely fine sizes in comparison to α-Al grains in the composite. All the poorly indexed points (black coloured) were excluded from the image as noise [42]. The grains were elongated due to semisolid forging with

particles aligned along the grain boundaries in the composite (Fig. 7(b)), while grains were found to be equiaxed in as cast composite (Fig. 7(a)).

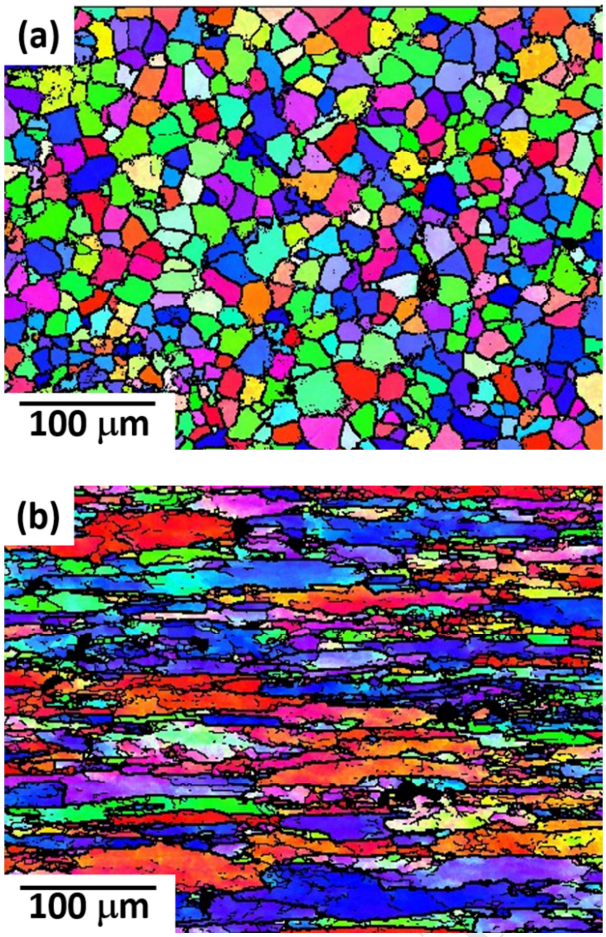

Fig. 7. EBSD map showing the grain orientation in Al-4.5Cu-5TiB_2 composite (a) as cast condition (b) $V_{f,\ liquid}$ = 0.3, 30% reduction.

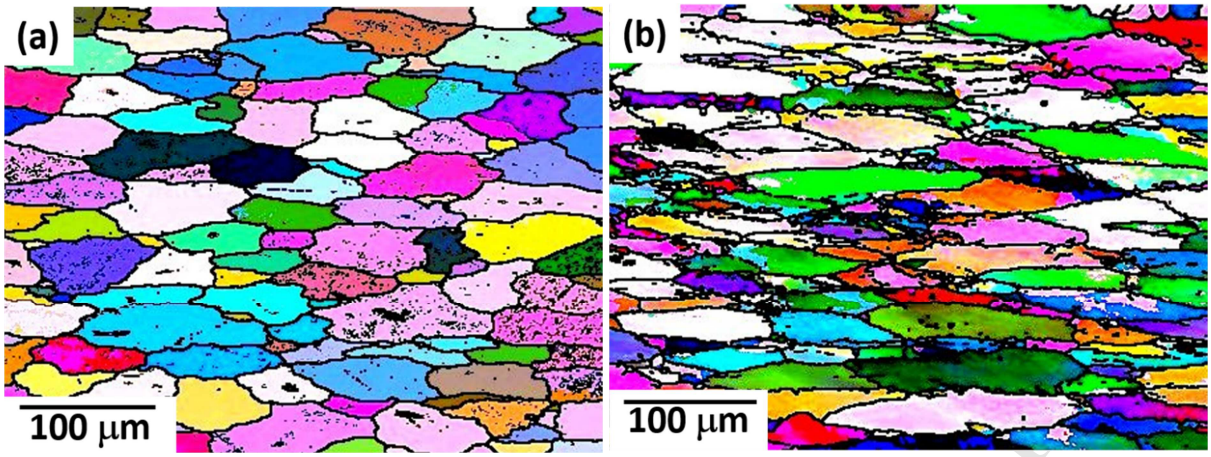

Fig. 8. EBSD map showing the grain orientation in Al-4.5Cu-alloys (a) as cast condition (b) $V_{f,liquid}$ = 0.3, 30% reduction.

Fig. 8 shows the grain orientaion in as cast alloy and semi solid processed in-situ Al-Cu alloy. The grains were observed to be elongated due to semisolid forging (Fig. 8(b)) as compared to the grains in as cast alloy (Fig. 8(a)). Fig 9 shows EBSD mapping representing the effect of semisolid forging on grain misorientation angle and grain size of the composite. The grain boundaries with a misorientation angle above 15° is generally considered as high angle boundaries (HAB), while grain boundaries with a misorientation angle below 15° are considered as low angle boundaries (LAB). As shown in Fig. 9(a) as cast composite has almost all of its grain boundaries as HAB with a higher degree of uniformity, while semisolid forged composite has significantly higher amount of LAB along with HAB. During hot deformation in semi solid state, liquid film forms at grain boundaries thereby causing migration of grain boundaries which initiated recrystallization in the alloy [43]. Some of the boundaries are incomplete LAB and mixed character which might be due to a transformation from low angle to high angle or vice versa. The mixed nature of boundaries is due to the continuous type recrystallization (CDRX) [42]. During dynamic recovery the LAB'S increases progressively results in formation of new grains which then transforms into HAB's [44]. As shown in Fig. 9(a) more than 95% grain boundaries were found to be high angle

boundaries in as cast composite, whereas only 60% of grain boundaries were found to be high angle boundaries in semisolid forged composite. Further, the grain size is found to be finer in the semisolid forged composite as compared to as cast composite (Fig. 9(b)).

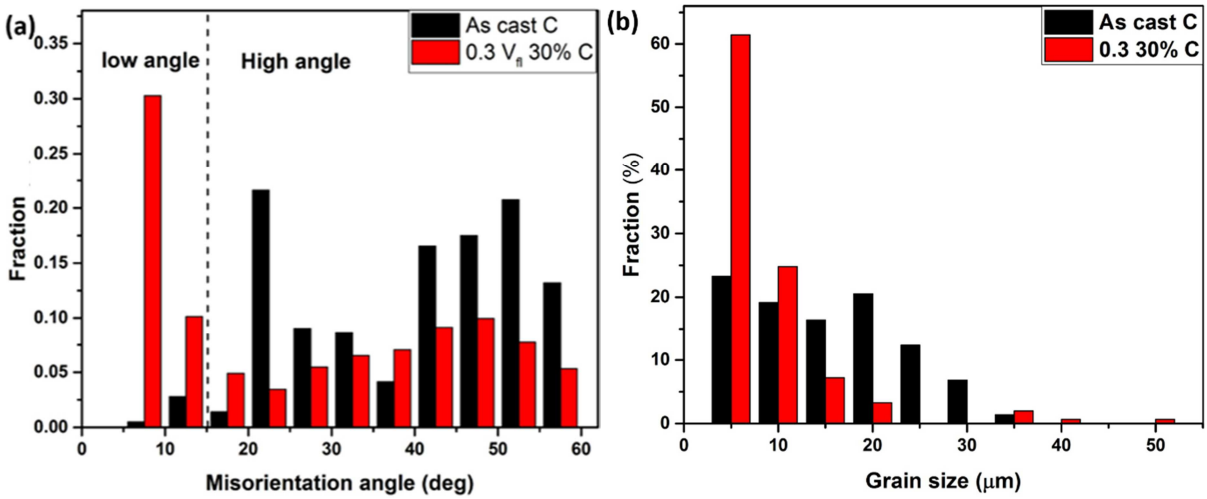

Fig. 9. EBSD results of Al-4.5Cu-5TiB_2 composite showing the effect of semisolid forging on (a) grain misorientation angle, and (b) grain size distribution.

A similar type of observation is obtained after semisolid forging of Al-4.5Cu alloy. Fig. 10 represents EBSD results showing the effect of semisolid forging on grain misorientation angle, and grain size distribution of Al-4.5Cu alloy. As shown in Fig. 10(a), more than 90% boundaries were found to be high angle boundaries in as cast alloy, whereas only 50% of boundaries are found to be high angle boundaries in semisolid forged alloy. Further, the grains in semisolid forged alloy were found to be fine in size as compared to as cast alloy (Fig. 10(b)).

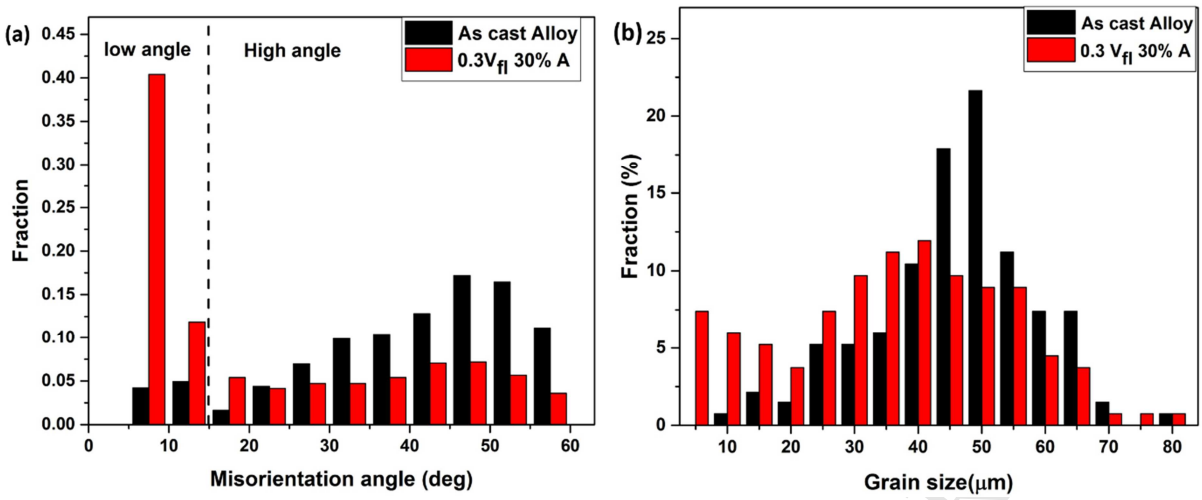

Fig.10. EBSD results of Al-4.5Cu alloy showing the effect of semisolid forging on (a) grain misorientation angle, and (b) grain size distribution.

Hence, above EBSD results as shown in Fig 9 and Fig 10 represent that the application of semisolid forging results in formation of fine new grains due to recrystallization in alloy and composite respectively. Similar observations were made by Hogg et al. [45] that the hot compression of aluminium alloys resulted in a grain refinement of microstructure by partial dynamic recrystallization in the alloy. The size of newly formed recrystallized grains depends on the nucleation rate and the velocity of moving HAB's [46]. The average grain size was found to be small in the alloy (Fig 10(b)) as compared to the composite (Fig 9(b)). Also, the effect of semisolid forging on grain size of the composite was found to be significantly higher than the alloy. The fraction of low angle boundaries formed due to semisolid forging of composite (Fig 9(a)) was found to be less than the fraction of low angle boundaries formed due to semisolid forging of the alloy (Fig 10(a)). The particles could have inhibited the movement of dislocations, initiated the heterogeneous nucleation and resulted in enhanced recrystallization. However, further studies need to be performed using TEM to understand the mechanism of dynamic recrystallization and moving of grain boundaries due to semi solid forging of alloys and composites.

3.4 Nanoindentation

The hardness and elastic modulus of as-cast and semi-solid forged Al-4.5Cu alloy and Al-4.5Cu-5TiB_2 composite were determined from the loading-unloading curve using the method proposed by Oliver and Pharr [38]. In order to minimize the indentation size effects, an indentation depth of 0.713 µm and an interval of 20 µm between each indentation was used [39,40]. Fig. 11 shows the loading - unloading curve of semi-solid processed Al-4.5Cu alloy and Al-4.5Cu-5TiB_2 composite from which the hardness and elastic modulus were measured.

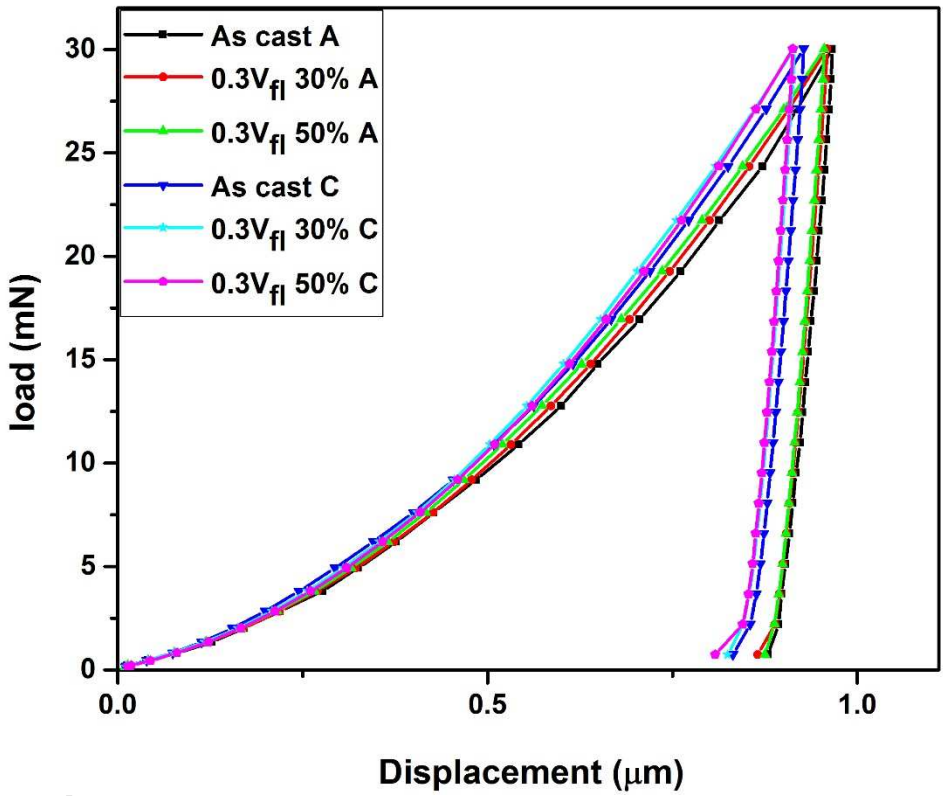

Fig. 11. Loading - unloading curve of semisolid processed Al-4.5Cu alloy and Al-4.5Cu-5TiB_2 composite.

The grain orientation differences have a significant effect on indentation measurements. Pathak et al. [47] studied the indentation behaviour of as cast and 30% deformed samples and

they reported a dramatic increase in modulus with increase in local dislocation and the local stored energy due to deformation. Table 1 summarizes the results of as cast and semi-solid forged Al-4.5Cu alloy and Al-4.5Cu-5TiB2 composite measured using nano indentation as shown in Fig. 11. The results show that the hardness of the alloy is increased on semisolid processing. The hardness of Al-4.5Cu alloy is increased by 2.14% after semisolid forging. This increase in hardness could be due to the closure of pores by the application of compressive force applied during forging and recrystallization of the grains. The hardness of as cast Al-4.5Cu-5TiB2 composite was increased by 7.14% compared to the as cast Al-4.5Cu alloy. This can be attributed to the reinforcement of TiB_2 particles in the composite [6, 20, 29]. Further, it was observed that the semisolid forging has a significant influence on the elastic modulus of the alloy and composite. The elastic modulus of as-cast Al-4.5Cu-5TiB_2 composite was found to be 9% higher than the as-cast Al-4.5Cu alloy. This increase in elastic modulus can be attributed to the reinforcement of TiB_2 particles in the matrix [48]. The elastic modulus and hardness is increased by 8% and 2.14 % respectively in case of alloy, while elastic modulus and hardness increased by 15% and 7.14% respectively in case of composite due to semi solid forging.

Table 1 :Elastic modulus and hardness of Al-4.5Cu alloy and Al-4.5Cu-5TiB_2 composite

Materials	Elastic modulus (GPa)	% increase	Hardness (GPa)	% increase
Al-4.5Cu alloy	89.68 ± 2.86	0	1.40 ± 0.06	0
Al-4.5Cu alloy, 0.3V_{fl}, 30% reduction	90.71 ± 3.51	1%	1.41 ± 0.07	0.07%
Al-4.5Cu alloy, 0.3V_{fl}, 50% reduction	97.35 ± 2.29	8%	1.43 ± 0.09	2.14%
Al-4.5Cu-5TiB_2 composite	97.99 ± 3.14	9%	1.50 ± 0.14	7.14%
Al-4.5Cu-5TiB_2 composite, 0.3V_{fl}, 30% reduction	111.33 ± 3.69	24%	1.60 ± 0.11	14.28%
Al-4.5Cu-5TiB_2 composite, 0.3V_{fl}, 50% reduction	108.70 ± 3.01	20%	1.55 ± 0.06	10.71%

Further, it was observed that the increase in forge deformation from 30% to 50% shows a significant change in the elastic modulus and hardness of the composite. The elastic modulus and hardness are found to be higher for the 30% reduction condition. The possible reason for this could be the better distribution of TiB_2 particles and reduction in cluster size when subjected to 30% deformation [49]. The cluster size reduction and TiB_2 particle distribution in Al-4.5Cu-5TiB_2 composite with 30% reduction by semisolid forging was well explained in our recent X-ray computed tomography studies [28]. Kuruvilla et al. [50] found that the extremely fine size TiB_2 particle reinforcements results in the improvement of elastic modulus of the aluminium matrix composite. This study shows the application of semi solid forging on improvement of mechanical properties of the alloy and composite by the combined effect of reinforcement of TiB_2 particles and enhanced dynamic recrystallization of alloy and composite.

4. Conclusions

The in-situ TiB_2 particles in Al-4.5Cu-5TiB_2 composite perform a dual role of grain refiner and reinforcement thus contributing to hardening by Hall-Petch mechanism as well as dispersion hardening mechanism. Semisolid forging of the composite leads to fragmentation of TiB_2 clusters thereby enabling uniform distribution of particles in the matrix. It also enables dynamic recrystallization and nucleation of grains with increased dislocation density. This leads to marked increase in hardness and elastic modulus of the alloy as well as the composite.

Acknowledgement

We would like to thank Director, CSIR-IMMT for giving permission to publish the nanindentation results. We would like to thank Dr Vit Janik, WMG, University of Warwick for his immense support in analysing the EBSD data.

6. References

[1] G. Hirt, R. Cremer, T. Witulski, H. Tinius, Lightweight near net shape components produced by thixoforming, Mater. Des. 18 (1998) 315–321. doi:10.1016/S0261-3069(97)00071-X

[2] J. V. Wood, P. Davies, J.L.F. Kellie, Properties of reactively cast aluminium–TiB_2 alloys, Mater. Sci. Technol. 9 (1993) 833–840. doi:10.1179/mst.1993.9.10.833.

[3] M.A. Herbert, R. Maiti, R. Mitra, M. Chakraborty, Wear behaviour of cast and mushy state rolled Al-4.5Cu alloy and in-situ Al4.5Cu-5TiB2 composite, Wear. 265 (2008) 1606–1618. doi:10.1016/j.wear.2008.03.010.

[4] R. MITRA and Y.R. Mahajan, Interfaces in discontinuously reinforced metal matrix composites : An overview, Bull. Mater. Sci. 18 (1995) 405–434. doi:10.1007/BF02749771.

[5] S.C. Tjong, Z.Y. Ma, Microstructural and mechanical characteristics of in situ metal matrix composites, Mater. Sci. Eng. R Reports. 29 (2000) 49–113. doi:10.1016/S0927-796X(00)00024-3.

[6] C.S. Ramesh, A. Ahamed, B.H. Channabasappa, R. Keshavamurthy, Development of Al 6063 – TiB_2 in situ composites, Mater. Des. 31 (2010) 2230–2236. doi:10.1016/j.matdes.2009.10.019.

[7] N. Hosseini, F. Karimzadeh, M.H. Abbasi, M.H. Enayati, Tribology International A comparative study on the wear properties of coarse-grained Al6061 alloy and nanostructured Al6061 – Al_2O_3 composites, Tribiology Int. 54 (2012) 58–67. doi:10.1016/j.triboint.2012.04.020.

[8] N. Soltani, H.R.J. Nodooshan, A. Bahrami, M.I. Pech-canul, W. Liu, G. Wu, Effect of hot extrusion on wear properties of Al – 15 wt .% Mg_2Si in situ metal matrix

composites, Mater. Des. 53 (2014) 774–781. doi:10.1016/j.matdes.2013.07.084.

[9] F. Toptan, A. Kilicarslan, A. Karaaslan, M. Cigdem, I. Kerti, Processing and microstructural characterisation of AA 1070 and AA 6063 matrix B_4C_p reinforced composites, Mater. Des. 31 (2010) S87–S91. doi:10.1016/j.matdes.2009.11.064.

[10] D. Jeyasimman, R. Narayanasamy, R. Ponalagusamy, V. Anandakrishnan, M. Kamaraj, The effects of various reinforcements on dry sliding wear behaviour of AA 6061 nanocomposites, Mater. Des. 64 (2014) 783–793. doi:10.1016/j.matdes.2014.08.039.

[11] B.S. Murty, S. A. Kori, M. Chakraborty, Grain refinement of aluminium and its alloys by heterogeneous nucleation and alloying, Int. Mater. Rev. 47 (2002) 3–29. doi:10.1179/095066001225001049.

[12] C. Bartels, D. R, G. Gottstein, U. Huber, Investigation of the precipitation kinetics in an A16061 / TiB_2 metal matrix composite, 237 (1997) 12–23. doi:10.1016/S0921-5093(97)00104-4.

[13] A. Jana, I.G. Siddhalingeshwar, R. Mitra, Effect of homogeneity of particle distribution on tensile crack propagation in mushy state rolled in situ Al-4.5Cu-5TiB_2 particulate composite, Mater. Sci. Eng. A. 575 (2013) 104–110. doi:10.1016/j.msea.2013.03.049.

[14] A. Mandal, R. Maiti, M. Chakraborty, B.S. Murty, Effect of TiB_2 particles on aging response of Al-4Cu alloy, Mater. Sci. Eng. A. 386 (2004) 296–300. doi:10.1016/j.msea.2004.07.026.

[15] R.G. Munro, Material Properties of Titanium Diboride, 105 (2000) 709–720.

[16] C. Zou, H. Kang, W. Wang, Z. Chen, R. Li, X. Gao, T. Li, T. Wang, Effect of La addition on the particle characteristics , mechanical and electrical properties of in situ Cu-TiB_2 composites, J. Alloys Compd. 687 (2016) 312–319. doi:10.1016/j.jallcom.2016.06.129.

[17] J. Geng, T. Hong, Y. Shen, G. Liu, C. Xia, D. Chen, M. Wang, H. Wang, Microstructural stability of in-situ TiB_2/Al composite during solution treatment, Mater. Charact. 124 (2017) 50–57. doi:10.1016/j.matchar.2016.11.032.

[18] Y. Birol, Semi-solid processing of the primary aluminium die casting alloy A365, J. Alloys Compd. 473 (2009) 133–138. doi:10.1016/j.jallcom.2008.05.074.

[19] A. Bolouri, M. Shahmiri, C.G. Kang, Study on the effects of the compression ratio and mushy zone heating on the thixotropic microstructure of AA 7075 aluminum alloy via SIMA process, J. Alloys Compd. 509 (2011) 402–408. doi:10.1016/j.jallcom.2010.09.042.

[20] I.G. Siddhalingeshwar, M.A. Herbert, M. Chakraborty, R. Mitra, Effect of mushy state rolling on age-hardening and tensile behavior of Al-4.5Cu alloy and in situ Al-4.5Cu-5TiB_2 composite, Mater. Sci. Eng. A. 528 (2011) 1787–1798. doi:10.1016/j.msea.2010.11.027.

[21] Y. Birol, Thixoforging experiments with 6082 extrusion feedstock, J. Alloys Compd. 455 (2008) 178–185. doi:10.1016/j.jallcom.2007.01.053.

[22] Z. Fan, Semisolid metal processing, Int. Mater. Rev. 47 (2002) 49-85. doi:10.1179/095066001225001076.

[23] J. Wannasin, R. Canyook, S. Wisutmethangoon, M.C. Flemings, Grain refinement behavior of an aluminum alloy by inoculation and dynamic nucleation, Acta Mater. 61 (2013) 3897–3903. doi:10.1016/j.actamat.2013.03.029.

[24] L.H. Liu, C. Yang, L.M. Kang, S.G. Qu, X.Q. Li, W.W. Zhang, W.P. Chen, Y.Y. Li, P.J. Li, L.C. Zhang, A new insight into high-strength $Ti_{62}Nb_{12.2}Fe_{13.6}Co_{6.4}Al_{5.8}$ alloys with bimodal microstructure fabricated by semi-solid sintering, Sci. Rep. 6 (2016) 23467. doi:10.1038/srep23467.

[25] Y. Chen, W. Yang, H. Zhan, F. Zhang, Y. Huo, Y. Zhao, X. Song, Y. Gu, Tailorable Burning Behavior of Ti14 Alloy by Controlling Semi-Solid Forging Temperature, Materials (Basel). 9 (2016) 697. doi:10.3390/ma9080697.

[26] R. Canyook, J. Wannasin, S. Wisuthmethangkul, M.C. Flemings, Characterization of the microstructure evolution of a semi-solid metal slurry during the early stages, Acta Mater. 60 (2012) 3501–3510. doi:10.1016/j.actamat.2012.03.002.

[27] D.C. Hofmann, S.N. Roberts, H. Kozachkov, Infrared thermal processing history of a Ti-based bulk metallic glass matrix composite manufactured via semi-solid forging, Acta Mater. 95 (2015) 192–200. doi:10.1016/j.actamat.2015.05.029.

[28] J. Mathew, A. Mandal, J. Warnett, M.A. Williams, M. Chakraborty, P. Srirangam, X-ray tomography studies on porosity and particle size distribution in cast in-situ Al-Cu-TiB_2 semi-solid forged composites, Mater. Charact. 118 (2016) 57-64. doi:10.1016/j.matchar.2016.05.010.

[29] S. Deepak Kumar, A. Mandal, M. Chakraborty, On the age hardening behavior of thixoformed A356–5TiB_2 in-situ composite, Mater. Sci. Eng. A. 636 (2015) 254–262. doi:10.1016/j.msea.2015.03.076.

[30] T. Sakai, H. Miura, A. Goloborodko, O. Sitdikov, Continuous dynamic recrystallization during the transient severe deformation of aluminum alloy 7475, Acta Mater. 57 (2009) 153–162. doi:10.1016/j.actamat.2008.09.001.

[31] S. Gourdet, F. Montheillet, An experimental study of the recrystallization mechanism during hot deformation of aluminium, Mater. Sci. Eng. A. 283 (2000) 274–288. doi:10.1016/S0921-5093(00)00733-4.

[32] P.B. Prangnell, C.P. Heason, Grain structure formation during friction stir welding observed by the “stop action technique,” Acta Mater. 53 (2005) 3179–3192.

doi:10.1016/j.actamat.2005.03.044.

[33] M. Mandal, R. Mitra, Effect of Mushy State Rolling on the Microstructure, Microhardness, and Microtexture in Al-4.5wt.%Cu-5wt.%TiB2 In Situ Composite, Jom. 68 (2016) 1902–1908. doi:10.1007/s11837-016-1911-4.

[34] J. Douin, S. Jouannigot, M. Zakhour, M. Nakhl, J. Silvain, J. Bobet, Materials Science & Engineering A Hardness and Young ' s modulus behavior of Al composites reinforced by nanometric TiB_2 elaborated by mechanosynthesis, 591 (2014) 1–8. doi:10.1016/j.msea.2013.10.065.

[35] S.S. Singh, C. Schwartzstein, J.J. Williams, X. Xiao, F. De Carlo, N. Chawla, 3D microstructural characterization and mechanical properties of constituent particles in Al 7075 alloys using X-ray synchrotron tomography and nanoindentation, J. Alloys Compd. 602 (2014) 163–174. doi:10.1016/j.jallcom.2014.03.010.

[36] Y.W. Bao, W. Wang, Y.C. Zhou, Investigation of the relationship between elastic modulus and hardness based on depth-sensing indentation measurements, Acta Mater. 52 (2004) 5397–5404. doi:10.1016/j.actamat.2004.08.002.

[37] S. Bajpai, A. Gupta, S.K. Pradhan, T. Mandal, K. Balani, Crack Propagation Resistance of α-Al2O3 Reinforced Pulsed Laser-Deposited Hydroxyapatite Coating on 316 Stainless Steel, Jom. 66 (2014) 2095–2107. doi:10.1007/s11837-014-1152-3.

[38] W.C. Oliver, G.M. Pharr, Measurement of hardness and elastic modulus by instrumented indentation: Advances in understanding and refinements to methodology, J. Mater. Res. 19 (2004) 3–20. doi:10.1557/jmr.2004.19.1.3.

[39] K.M. Mussert, A nano-indentation study on the mechanical behaviour of the matrix material in an AA6061 - Al_2O_3 MMC, Jom. 7 (2002) 789–794. doi:10.1023/A:1013896032331.

[40] X. Li, B. Bhushan, A review of nanoindentation continuous stiffness measurement technique and its applications, Mater. Charact. 48 (2002) 11-36. doi:10.1016/S1044-5803(02)00192-4.

[41] J. Sun, X. Zhang, Y. Zhang, N. Ma, H. Wang, Effect of alloy elements on the morphology transformation of TiB_2 particles in Al matrix, Micron. 70 (2015) 21–25. doi:10.1016/j.micron.2014.12.002.

[42] D. Yadav, R. Bauri, Friction Stir Processing of Al-TiB_2 In Situ Composite: Effect on Particle Distribution, Microstructure and Properties, J. Mater. Eng. Perform. 24 (2015) 1116–1124. doi:10.1007/s11665-015-1404-6.

[43] H. V. Atkinson, K. Burke, G. Vaneetveld, Recrystallisation in the Semi-Solid State in 7075 Aluminium Alloy, Int. J. Mater. Form. 1 (2008) 973–976. doi:10.1007/s12289-008-0220-z

[44] S. Gourdet, F. Montheillet, A model of continuous dynamic recrystallization, Acta Mater. 51 (2003) 2685–2699. doi:10.1016/S1359-6454(03)00078-8.

[45] S.C. Hogg, I.G. Palmer, L.G. Thomas, P.S. Grant, Processing, microstructure and property aspects of a spraycast Al-Mg-Li-Zr alloy, Acta Mater. 55 (2007) 1885–1894. doi:10.1016/j.actamat.2006.10.057.

[46] C. Sommitsch, W. Mitter, On modelling of dynamic recrystallisation of fcc materials with low stacking fault energy, Acta Mater. 54 (2006) 357–375. doi:10.1016/j.actamat.2005.09.008.

[47] S. Pathak, D. Stojakovic, S.R. Kalidindi, Measurement of the local mechanical properties in polycrystalline samples using spherical nanoindentation and orientation imaging microscopy, Acta Mater. 57 (2009) 3020–3028. doi:10.1016/j.actamat.2009.03.008.

[48] H. Yi, N. Ma, Y. Zhang, X. Li, H. Wang, Effective elastic moduli of Al-Si composites reinforced in situ with TiB_2 particles, Scr. Mater. 54 (2006) 1093–1097. doi:10.1016/j.scriptamat.2005.11.070.

[49] D.J. Lloyd, Particle reinforced aluminium and magnesium matrix composites, Int. Mater. Rev. 39 (1994) 1–23. doi:10.1179/imr.1994.39.1.1

[50] A.K. Kuruvilla, K.S.Prasad, V.V.Bhanuprasad, Y.R.Mahajan, Microstructure-property correlation in Al/TiB_2(XD)composites Scr. Mater. 24 (1990) 873-878. doi:10.1016/0956-716X(90)90128-4

Effect of semi-solid forging on microstructure and mechanical properties of in-situ Al-Cu-TiB_2 composites

Highlights:

- Al-Cu-TiB_2 MMC was prepared by casting using flux assisted synthesis method.
- Semisolid forging was employed to deagglomerate TiB_2 clusters in the composite.
- Semisolid forging resulted in improvement in grain refinement in the composite due dynamic recrystallization.
- 30% forge reduction in semi solid state improved young's modulus and hardness of the composite.